THE PHOTOGRAMMETRIC RECORD

The Photogrammetric Record 31(155): 304–324 (September 2016)
DOI: 10.1111/phor.12155

MONITORING 3D VIBRATIONS IN STRUCTURES USING HIGH-RESOLUTION BLURRED IMAGERY

DAVID M. J. MCCARTHY (d.mccarthy@lboro.ac.uk)
JIM H. CHANDLER (j.h.chandler@lboro.ac.uk)
ALESSANDRO PALMERI (a.palmeri@lboro.ac.uk)
Loughborough University, Loughborough, UK

Abstract

Photogrammetry has been used in the past to monitor the laboratory testing of civil engineering structures using multiple image-based sensors. This has been successful, but detecting vibrations during dynamic structural tests has proved more challenging because they usually depend on high-speed cameras which often results in lower image resolutions and reduced accuracy. To overcome this limitation, a novel approach has been devised to take measurements from blurred images in long-exposure photographs. The motion of the structure is captured in individual motion-blurred images without dependence on imaging speed. A bespoke algorithm then determines each measurement point's motion. Using photogrammetric techniques, a model structure's motion with respect to different excitation frequencies is captured and its vibration envelope recreated in 3D. The approach is tested and used to identify changes in the model's vibration response.

KEYWORDS: close range photogrammetry, deformation, engineering, motion blur, structural health monitoring, vibration

INTRODUCTION

CIVIL ENGINEERING STRUCTURES often need to be tested to verify their performance and integrity. This requires meticulous planning so that sufficient data is collected with a sufficient number of carefully positioned sensors. Contact transducers are often used, though they have certain limitations, particularly if access to the structure is difficult. In the case of structural testing using dynamic test techniques, advanced sensors allow more detailed measurement. This approach is particularly convenient as the presence of damage tends to result in a localised change in the stiffness within the structure, which can then affect the vibration response elsewhere.

The advantages of photogrammetry can be realised when applied to structural testing as a very high number of points can be recorded with few sensors, without any contact with the structure. This is of primary relevance when measuring dynamic-mode shapes, since interpolation is necessary between each measuring point. Current hardware, however, limits the potential for this type of dynamic monitoring, which necessitates much higher imaging speeds.

In this paper, a novel approach is developed to directly measure the blur created by a deliberately long exposure. This is explained and tested after the importance of structural testing and prior work is reviewed. The approach has built on previous developments (McCarthy et al., 2013, 2014) and the results of enhanced case studies are included here.

Structural Testing

Assessments of structural integrity are often necessary for a variety of reasons. New materials under development in a laboratory environment may demand complex monitoring schemes to understand deformation patterns. Testing may also be prescribed during construction as verification of some critical elements. Testing of existing structures may be needed for evaluation prior to a change of use, or following a potentially damaging event. Long-term structural health monitoring schemes are necessary on some structures to detect any potential deterioration.

Conventional structural tests apply an increasing load to a structure while its performance is monitored by gauges. Subject to acceptable results, the structure is then deemed suitable for its working loads. The load would be applied with, for example, test weights on a slab or large vehicles on a bridge. This testing of "static" structural properties may be considered inconvenient since the test would necessitate taking the structure out of service, in addition to the logistical problems of transporting and moving loads. Care must also be taken to not increase the load above the structure's elastic limit, otherwise damage may occur from the test itself.

Dynamic structural monitoring is now emerging as a viable and effective approach for assessing structural performance (Brownjohn, 2011). Data collection is considered more convenient since much lower loading is necessary and monitoring can take place without the structure being out of service. However, data analysis can be complicated and specialist expertise is necessary to interpret the vibration response. Several approaches exist to identify structural changes from the measured vibration response (Kasinos et al., 2015). Comparative studies score these approaches on their ability to identify, locate and quantify damage; generally, those approaches which take advantage of a higher number of monitoring points produce the most reliable results (Carden and Fanning, 2004).

Monitoring of Structural Tests

Engineers must select and distribute sensors appropriately to collect sufficient data to understand forces and deformations within a structure. Traditional contact sensors measure displacements or strains. For example, linear variable-displacement transducer (LVDT) sensors can be used to measure displacement at various points on a structure, usually at a beam's mid-span or other equally spaced locations. Foil strain gauges measure strain in the material, the dimensionless measure of extension in a given direction.

Traditional contact gauges are reliable, well understood and often prescribed by engineers, but in many cases their effectiveness is limited by the fact that they only record the structure's performance at a single location, namely, the position where they are fitted. The possibility of individual gauges being affected by local variations in the material or local strain concentrations should be recognised. Strain gauges are also susceptible to daily and seasonal environmental changes, being a significant limiting factor in long-term structural health monitoring. Furthermore, each additional sensor costs money, takes time to fit and requires cabling infrastructure, and many sensors only measure in one dimension unless the more expensive multidimensional counterparts are used. Harvey (2008) noted the

importance of carefully locating sensors, as a poorly sited sensor may not measure anything useful.

More advanced non-contact sensors can be used, including a total station or terrestrial laser scanner. These sensors can collect optical measurements from several monitoring points, but both these instruments are unable to measure truly instantaneous point deformation. In addition, they take time to traverse the whole structure, making them suitable for testing of static properties only (Psimoulis and Stiros, 2008; Rönnholm et al., 2009). Differential GPS can monitor deformation without line-of-sight restrictions, but each individual monitoring point adds considerable cost (Roberts et al., 2004). The laser Doppler vibrometer (LDV) is a specialised optical dynamic sensor for monitoring vibrations. Changes in the wavelength of a reflected laser beam are related to the velocity of a moving surface. The instrument is very precise, but measures only at the location it is targeted at.

Photogrammetry has demonstrated its potential for monitoring structural tests in the past (Cooper and Robson, 1990; Maas, 1998; Benning et al., 2004). In particular, it allows instantaneous measurement of a very high number of monitoring points with a single arrangement of image sensors. These points may be monitored in 3D if using stereo or multiview imagery, whereas many contact gauges are one-dimensional, or have more expensive 3D variants. Other advantages include the fact that the method is non-contact, meaning that the monitoring instruments do not add load to the test subject, and a stable reference on which to support contact gauges is not required. In particular, the photogrammetric approach is scalable and suitable for a wide range of applications from small-scale laboratory tests (Thomas and Cantré, 2009) to full-size structures.

Photogrammetry has also been shown to be suitable for monitoring dynamic tests. Since all monitoring points within an image are measured simultaneously, additional points can be added, and the distance between each monitoring point reduced, with little additional cost. Vibrations can be captured by increasing imaging speed to many frames per second (fps). The Nyquist sampling theorem dictates that, in order for certain frequencies to be detected, data must be sampled at at least twice the desired frequency range. Olaszek (1999) notes that an even higher sampling frequency may be desirable since, even if the Nyquist theorem is satisfied, aliasing effects can cause the peak amplitude in the frequency domain to be missed.

Structural engineers always desire measurements that are as accurate as possible. Clearly, the use of the highest resolution cameras is desirable to achieve the highest precision measurement but, as noted above, high imaging speed is normally necessary to capture, and hence measure, vibration at the required frequencies. When selecting camera hardware for monitoring tests of static properties (which take place over several minutes or a few hours), potential speed of continuous imaging may not need to be considered. In contrast, for dynamic tests with relatively fast variations in the deformed state of the structure, consideration must be given to both the image resolution and the potential continuous imaging speed of the camera.

When selecting a camera, current sensor hardware requires a compromise to be made between the image resolution and temporal resolution of the sensor. Digital single-lens reflex (DSLR) cameras are available with image resolutions over 30 Mpixel and consumer camcorders typically record at up to 60 fps. However, a DSLR camera at its highest resolution setting can only sustain, at most, a few images per second. Consumer camcorders acquire images at higher frequencies, but only capture data at much lower image resolutions, typically 2·1 Mpixel (so-called high definition or "HD" resolution). Specialist machine-vision camera sensors exist in a wide variety of configurations, but even these sensors are limited by a trade-off between spatial resolution and imaging frequency, and are

expensive. Although the capabilities of image sensors are continually improving, so too do the demands of engineering researchers.

Real-time monitoring is very often desired for monitoring structural tests, since the engineer can appreciate the structure's performance as the tests takes place. When high-speed imaging is used for monitoring, the images must be processed at the same rate that they are acquired, otherwise the real-time detectable vibration frequencies are limited by the processing speed. Real-time monitoring at acceptable speeds is possible, but only at a reduced image resolution and hence reduced spatial accuracy or by reducing the number of points (Jurjo et al., 2010), increasing undesirable interpolation.

Capturing a very large number of high-resolution images also has practical difficulties. A considerable amount of data is generated and bottlenecks exist when images are stored to an internal memory card, uploaded to external file storage or to another computer for processing. If images are post-processed, or are to remain as documentary evidence, a large amount of data storage space is required.

Proposed Measurement Approach

Aimed at alleviating this penalising compromise between image resolution and imaging frequency, a radically new approach is presented in this paper, in which structural vibration is captured within long-exposure images. Indeed, the motion of the vibrating structure causes localised blur within the image, and this can be measured using automated image-processing methods.

Motion-blurred imagery has been examined in photogrammetry (for example, Sieberth et al., 2014). In the computer science literature, many algorithms have been published for extracting data from these seemingly poor-quality images (Yitzhaky et al., 2000; Wang et al., 2007). It is often assumed that a motion-blurred image is created from an ordinary sharp scene which is degraded by some blurring function. This blurring can be expressed using (Banham and Katsaggelos, 1997):

$$\mathbf{Y}(i,j) = \sum_{k=1}^{m} \sum_{l=1}^{n} \mathbf{H}(i,j;k,l)\mathbf{F}(k,l) + \mathbf{N}(i,j) \tag{1}$$

where for a pixel (k, l) in a sharp image and (i, j) in the corresponding blurred image: $\mathbf{F}(k, l)$ is an ordinary $m \times n$ sharp image; $\mathbf{H}(i, j; k, l)$ is the point spread function (PSF); $\mathbf{Y}(i, j)$ is the resultant blurred image; and $\mathbf{N}(i, j)$ represents noise.

The PSF, $\mathbf{H}$, contains information about the motion that caused the blur, including its extent, direction and distribution. Some algorithms are capable of *blind deconvolution*, that is, recovering the PSF without prior knowledge of the motion that caused the blur.

In the current implementation, an algorithm measures the motion blur exhibited by ordinary circular targets (McCarthy et al., 2014). Both the amplitude of the motion causing the motion blur and direction of the motion path are measured. A sinusoidal motion is assumed, as is expected during frequency-selective dynamic structural testing (Clough and Penzien, 2003; Chopra, 2007; Palmeri and Lombardo, 2011). Black circular targets with a white background are arranged at necessary monitoring points on the test subject in the conventional way. This implementation also requires a single sharp image of the test structure from the same cameras. This may be taken before dynamic excitation is applied or, in the case of a structure with environmental loading which vibrates continuously, simply an image taken with an appropriately fast shutter speed.

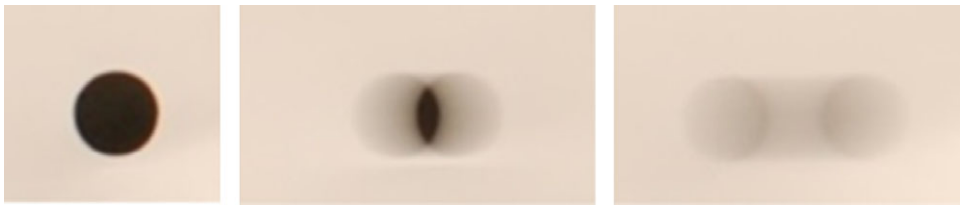

Fig. 1. Appearance of motion-blurred circular targets. Left: circular target without motion. Blurred images when the motion amplitude is either less than (centre) or greater than (right) the diameter d of the circular target.

When the test structure vibrates, either artificially by manually applying force or naturally under environmental loads such as wind, a single long-exposure image is taken. As a result, the whole vibration of the structure during the time that the shutter is open is captured within the single image. The motion amplitude and direction at each monitoring point can then be measured by processing these long-exposure images with a bespoke algorithm, implemented in MATLAB.

A set of preliminary tests were carried out on circular targets, which have demonstrated that their blurred images take a consistent form, exhibiting the same edges, shapes and gradients. Interestingly, two cases exist whereby the motion amplitude is either less than, or greater than, the diameter of the circular target (Fig. 1). In the former case, a small region of the image is continually occupied by the target throughout the exposure, and the pixels in this region remain at the same intensity as the black sharp target exhibiting no motion. Other image pixels, which are occupied by the target for only part of the whole exposure, generate a pixel value between that of the black target and the white border, proportional to the amount of time occupied by the target over that particular pixel. In the latter case, every region of the image is exposed to the white target border for at least some of the time that the shutter is open, so the pixel value measured by every pixel within the blurred target image is in between the black of the target and white of the target background.

Image-processing Procedure

The key steps in the bespoke image-processing algorithm are summarised in Fig. 2. The proposed procedure uses MATLAB's image-processing toolbox. Three measurements are estimated using different techniques, each achieving increasing accuracy, but at decreasing speed: (1) rapid approximate measurement; (2) pixel intensity profiles; and (3) iterative refinement.

Rapid Approximate Measurement

The blur-measurement algorithm assumes the approximate location of each target is already known, since blurred targets in an image are more difficult to locate than a sharply defined target. This is achieved by detecting targets in the additional sharp image, in which circular targets are easily identified, and a list of coordinates passed to the blur-measurement algorithm.

After locating the image patch of the blurred target, a rapid approximate estimate about the geometry of the image is determined with a simple thresholding algorithm. The chosen

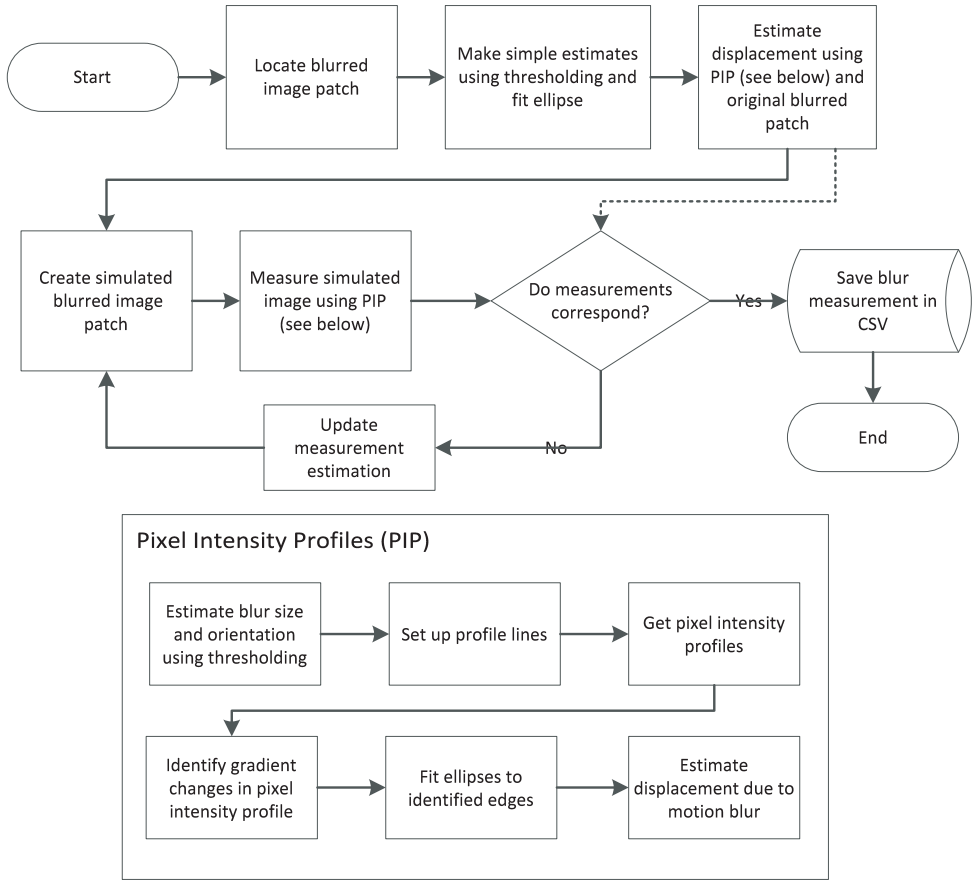

FIG. 2. Blur measurement calculation flowchart. PIP is pixel intensity profiles; CSV is comma separated values.

threshold needs to be nearer in value to the white of the target background, so that the detected region includes the grey regions at the edge of the blurred target. An ellipse is fitted to the detected region using least squares; the estimated major and minor axes and ellipse orientation allows arrangement of the profile lines for the next stage (Fig. 3).

Pixel Intensity Profiles

Secondly, parallel *pixel intensity profiles* (PIPs) are extracted from the image through the major axis of the blur. The PIP process is adapted from an approach proposed by Boracchi et al. (2007). The number of profiles can be adjusted, but 20 was found to be a suitable balance between measurement accuracy and processing time. An example PIP is shown in Fig. 4(b) (the signal is inverted so that target pixels result in a peak), and points can be identified at abrupt changes in the gradient of the intensity profile which relate to features on the blur smear (Fig. 4(a)). The algorithm identifies these features twice, differentiating the intensity profile and locating peaks in the resulting function. These features are allocated to two groups (shown in red and blue in Fig. 4), depending on whether

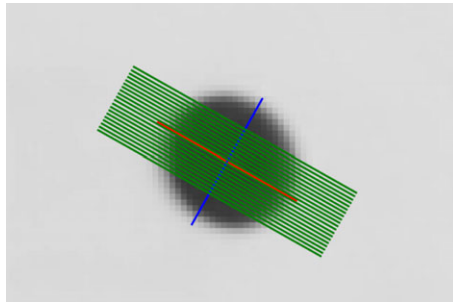

Fig. 3. Major and minor axes (red and blue) of the target with arranged pixel intensity profile lines (green).

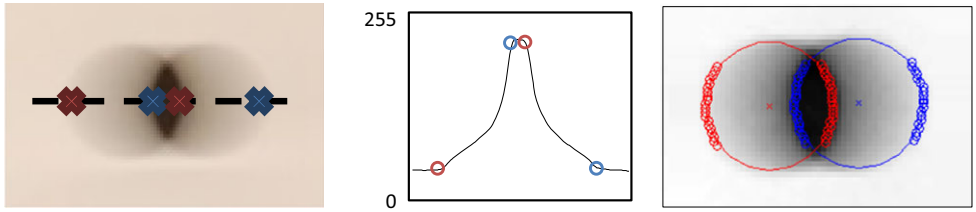

Fig. 4. Resultant blur measurement. Red and blue are the two feature groups depending on whether they follow or precede positive or negative gradients. Points identified in (a) are at the abrupt changes in the gradient of the intensity profile in (b). Ellipses are fitted to the two group of points in (c).

they follow or precede positive or negative gradients; ellipses are then fitted to each group of points (Fig. 4(c)). The distance and angle between the centre coordinates of these ellipses are taken as the estimated motion occurring at that monitoring point on the structure. Tests demonstrated that this method provides pixel-level accuracy of the motion amplitude.

The PIP algorithm is effective in both cases, where motion amplitude is both smaller and larger than the target diameter (Fig. 1); the algorithm identifies changes in gradient rather than changes in absolute pixel value. The type of blurred target is automatically identified by the presence of the dark central region, since this has an effect on the allocation of feature points in the PIPs into the two ellipses.

In tests, the PIP method alone regularly overestimated the exhibited motion and did not provide adequate accuracy due to a specific systematic effect. Motion was overestimated because at the edge of targets there is a gradient in pixel values, caused by chromatic aberration and lens diffraction. This was evident when an image of a stationary target exhibited an apparent displacement of approximately 1 pixel. A subsequent third step was therefore included to improve accuracy.

Iterative Refinement

To achieve superior accuracy an iterative procedure was introduced. Here, a simulated blurred image patch is generated using the blur function (equation (1)), using a sinusoidal PSF of the first estimated motion and the sharp image taken earlier. The equation used to describe the PSF, **H**, is defined by:

$$f(x) = \begin{cases} 0, & x < \frac{L-1}{2}; \\ \cos\frac{2\pi x}{L} + 1, & \frac{L-1}{2} \leq x \leq \frac{L+1}{2}; \\ 0, & x > \frac{L+1}{2}; \end{cases} \quad (2)$$

where L is the estimated motion amplitude. This function is discretised into units of a pixel by applying the trapezium rule over pixel intervals. The result of this function is spatially rotated by the estimated motion angle using MATLAB's *imrotate* function set to use bilinear interpolation. Finally, the matrix is divided by the sum of its elements, so that the elements of the final **H** sum to unity.

Pixel intensity profiles of this simulated image are measured and compared with the actual (as-taken) blurred image. If the initial measurement was correct, the actual and simulated image would correspond closely. If a discrepancy between the two remains, the amplitude and angle parameters of the PSF are iteratively adjusted by the measurement discrepancy until the difference between the measured motion in both the original and simulated image patches is less than a user-defined threshold (Fig. 5). The motion amplitude and angle used to create a simulated image that matched the actual image is then accepted as the vector describing the distance and direction of the motion at that point on the test subject.

Transformation into Object Space

Having measured image coordinates in pixel units, the distance and direction can be immediately represented graphically by superimposing displacement vectors onto the original images. By also superimposing the envelope of the motion, the output is similar to that produced by finite-element software packages that might be used to predict forces and deformations in the structure. By showing displacement vectors together with an image of the structure, the engineer can appreciate which parts of the structure have the greatest motion, as well as observing the distribution (and possibly spot any anomaly).

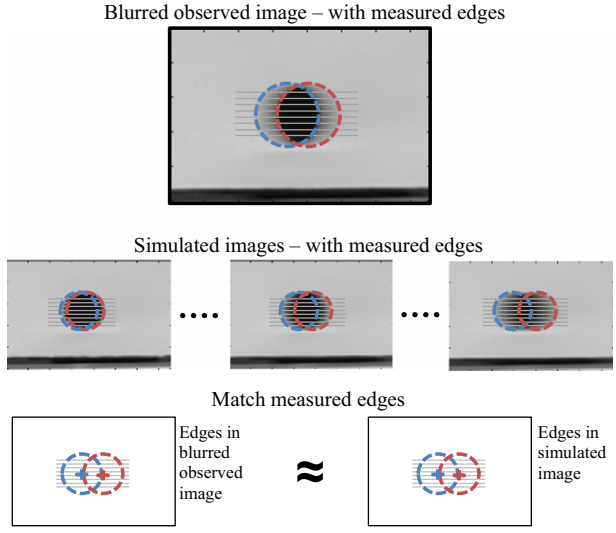

Fig. 5. Iteratively improving the accuracy using both the original blurred and simulated image patches.

2D Planar Measurement

It is also likely that an engineer would desire that these measurements are transformed into an appropriate object-space system (in millimetres) for more precise comparisons and analysis. With only a single camera, it is possible to provide 2D measurements so long as it is known that any movement is planar and the focal plane of the camera is aligned approximately with the same plane. In this scenario, a perspective transformation (Luhmann et al., 2006) can be used to transform coordinates from image space to object space. However, if any out-of-plane movement were to occur, this could cause a scaling error in the measured results. It is recognised that radial and tangential distortion cause a displacement of a projected object point in the image plane. However, if individual monitored points are displaced relative to a fixed camera, then computed object displacements are almost identical, whether a lens model is explicitly incorporated or not. However, the effects of lens distortion can be easily corrected following camera calibration (Luhmann et al., 2006) and a correction for this systematic effect should be incorporated.

Coded control targets can simply be arranged around the test object (coplanar to the monitoring targets) and their object-space coordinates measured using a reflectorless total station. Coordinates in an arbitrary 3D object-space (X, Y, Z) system are calculated. For calculating planar deformations, 2D plane-space (x, y) coordinates for each control point are determined (Fig. 6). The plane is defined by the object-space X and Y coordinates, to which linear regression is used to define an object-space plan gradient and intercept. The distance from the intercept to the nearest point along the regression line of each control point is taken as its plane-space x coordinate. The earlier determined object-space Z coordinates become corresponding plane-space vertical y coordinates. Projective transformation parameters are determined with the paired plane-space and image-space control target coordinates, which are used to apply the projective transform to the earlier measured image-space monitoring point coordinates.

Measurement in 3D

3D measurement has been highlighted in the past as a strength of photogrammetric methods for the monitoring of structures. The monitoring approach was expanded to fully 3D measurement that also allows non-planar motion to be recorded (McCarthy et al., 2014).

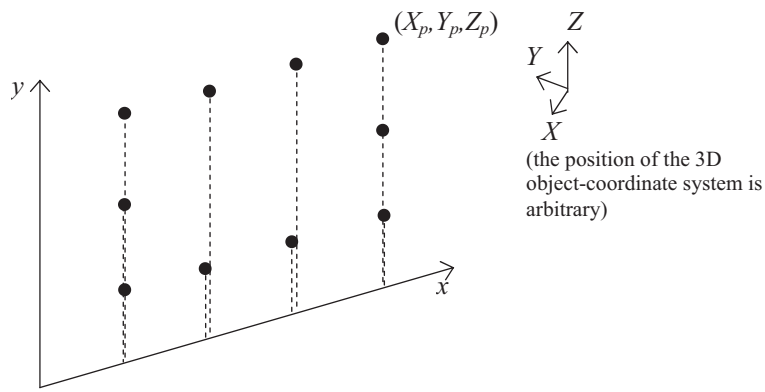

Fig. 6. Definition of 2D planar coordinates from 3D control point coordinates.

For a moving target, two 3D object points will be created on any image, representing the target at each "end" (limits) of its motion. A 3D approach requires the use of two or more sensors and their shutters must be interconnected so that they capture images simultaneously. Additional calculation steps for finding 3D coordinates are shown in Fig. 7.

The exterior orientation (EO) of the cameras needs to be known and was achieved using the PhotoModeler software package (version 2013.0.3.113 64-bit, July 2013; Eos Systems, Vancouver, Canada). This software is convenient because it automatically recognises coded control targets in images, and object-space coordinates for the control points can be loaded using a PhotoModeler coded coordinate file. PhotoModeler's automated camera calibration was also used to determine appropriate interior orientation (IO) parameters, including deriving an appropriate lens model, allowing accurate coordinates for the monitoring points to be determined. These object points allow approximate image coordinates to be computed, which are then used by the blur-measurement algorithm to assist locating targets in images. Target matching can also be carried out by PhotoModeler.

Image coordinates for the motion-blurred targets are measured as before using the image-processing algorithm described above and stored in a comma separated values (CSV) file. As mentioned above, a new challenge at the point-matching stage occurs since each target, which would normally have a single measurement in each image, instead has two coordinates measured at either end of its motion path. Unlike traditional photogrammetry, the image coordinates relating to a 3D point cannot be uniquely matched with coded targets since they originate from one physical target which changes position. Fig. 8 shows how two image coordinates exist for each target and how different pairs of candidate object points can be created.

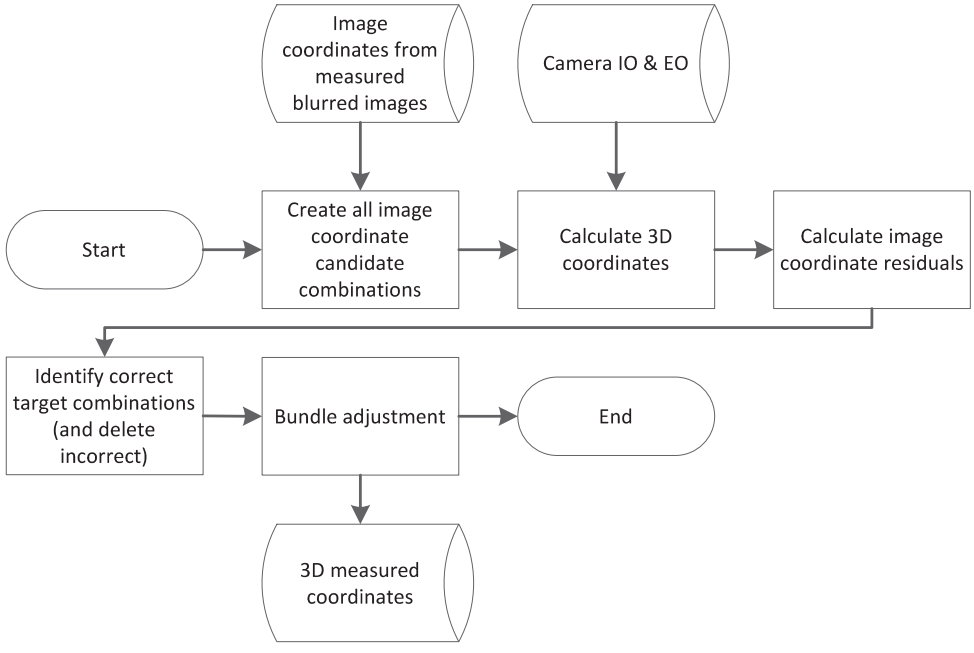

FIG. 7. 3D calculation flowchart.

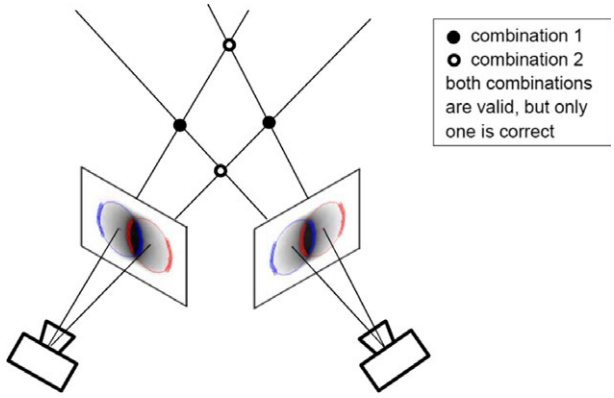

Fig. 8. Point-matching difficulties for a single blurred target.

To solve this ambiguity for all objects/camera-configurations, two candidate combinations of the pairs of coordinates for each target should be considered, since it is not yet known which combination is correct. 3D coordinates are therefore calculated for both combinations using a bespoke space-intersection program, using PhotoModeler's earlier derived EO and IO, which explicitly corrects for lens distortion. Residual image coordinates for the incorrect combination are usually significantly higher, depending on the exact arrangement (although, where the direction of target motion approaches the epipolar plane, they become similar, as discussed below). Residual coordinates are then calculated through reprojection of the 3D point onto the image, using the known camera orientations. In tests, it was found that selecting the combination of image coordinates which produces the smallest residual measurements overall, usually identified the correctly matched pair.

Although this method has proven to be generally successful, in a particular case the correct combination cannot be automatically determined; namely, where the orientation of both measured points lie on the same epipolar plane. It may be possible to determine the most likely combination using engineering judgement, but if "a priori" knowledge of the likely motion is available, then the two cameras can be arranged obliquely, such that this situation does not occur. It is therefore helpful to consider the likely target movement direction when selecting camera positions. This ambiguity could also be solved by adding a third camera to the system, although there would then be a $2^3 = 8$ combination of coordinates to consider for a single target.

Once 3D coordinates are determined, all the data was then input into a bundle adjustment (General Adjustment Program (GAP), Chandler and Clark, 1992) to calculate final 3D coordinates in object space.

Practical Tests and Results

A one-dimensional shaker table was used to test and demonstrate the proposed approach. The APS "Electro-Seis" 400 is a long-stroke shaker capable of carrying out programmed one-dimensional motions up to 150 mm as described in McCarthy et al. (2013, 2014). In its normal use, models are fitted to the 455 mm × 455 mm table bed which is programmed with vibrations of varying frequencies and amplitudes. As the model is

subjected to base vibration, data would be recorded about the model's dynamic response using accelerometers and a laser displacement gauge.

Two Nikon D80 DSLR cameras were available for image capture, each camera equipped with 24 mm fixed focal-length lenses and the focus fixed at the appropriate distance (Fig. 9(a)). The cameras have a sensor resolution of 10·2 Mpixel. The shutter speed was fixed at 1 s in order to capture the whole vibration cycle, and the aperture and sensitivity were set to f/32 and ISO 100 to provide clear images with appropriate contrast.

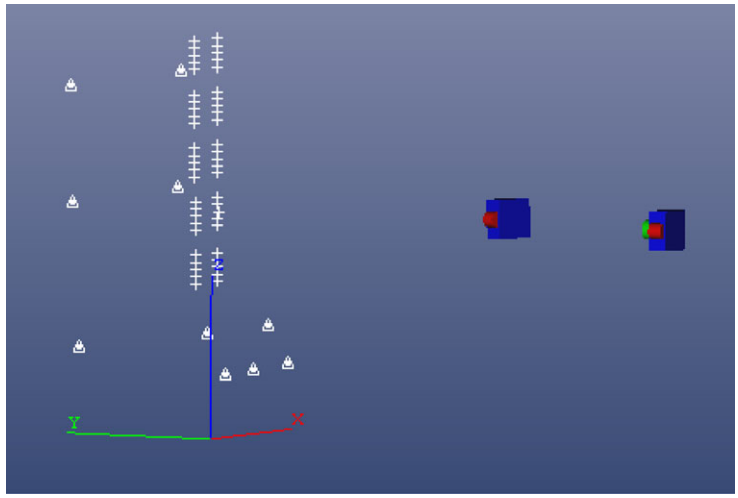

(a)

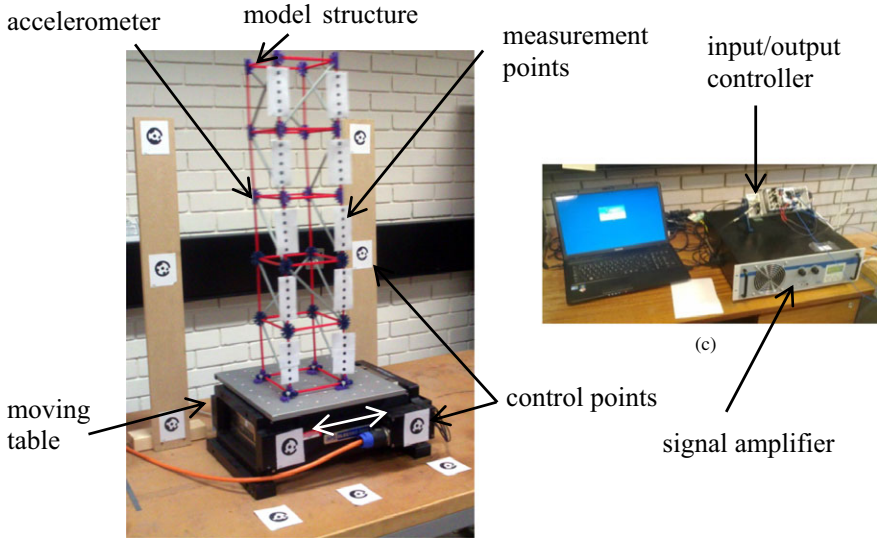

(c)

(b)

FIG. 9. (a) Experimental set-up. (b) Detail of vibration test subject. (c) Detail of shaker table control system.

The external shutter release for each camera was connected to the shaker table's control system (Fig. 9(c)) so that the exact time they are triggered is recorded alongside the sensor data so that a direct comparison can be made.

Simple plastic model structures with a height of 760 mm were rigidly fixed with bolts to the shaker table (Fig. 9(b)). The columns on the structure were marked with circular targets. Black 8 mm circles were printed on white paper backing with sufficient white space around the target so that the white space was sure to exceed the expected motion amplitude. Conventional coded targets were arranged around the shaker table to provide control points, and their positions were measured by a total station in reflectorless mode. For 2D monitoring, these must be in the same plane as the monitoring targets, whilst for 3D tests these define a volume occupied by the model structure.

Testing 2D Monitoring

For the first test, 2D measurements were made with a single camera positioned in front of the structure. The model structure was subjected to one-dimensional motion of varying frequencies. In particular, the model was excited with sinusoidal vibration at its natural frequencies (established separately using an accelerometer with a "sine sweep" input table motion) so that the model would exhibit its vibration envelope for these modal frequencies. These are of interest for looking at the curvature of the vibration envelope, and locating nodes and antinodes (Abdel Wahab and de Roeck, 1999). Fig. 10 shows recorded images overlain with the 2D measurements established using the image-processing routine previously described in the section 2D *Planar Measurement*. Three modes were used with the vibrations set to frequencies of 5, 8 and 12 Hz.

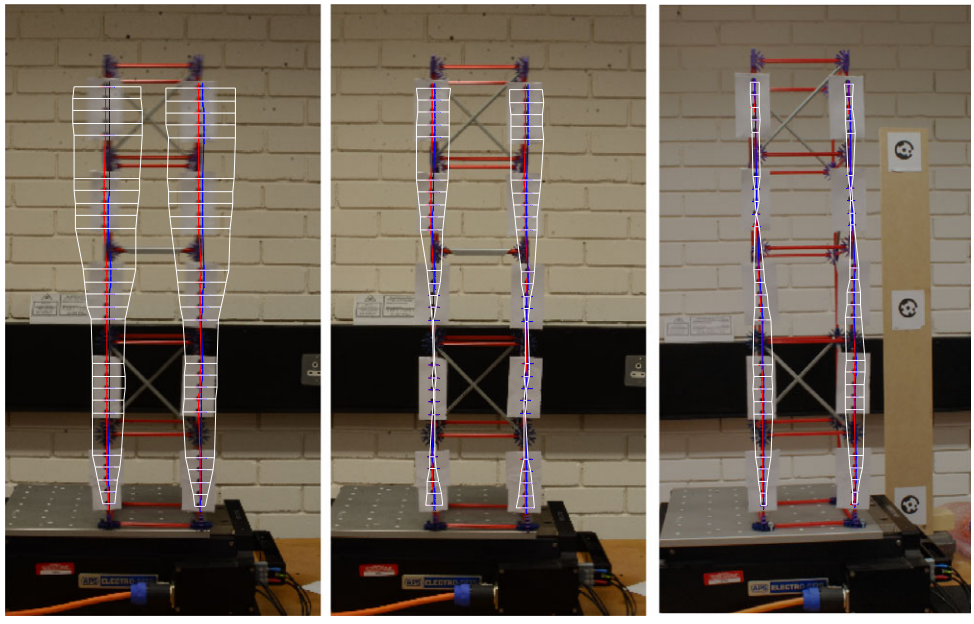

1st mode (5 Hz) 2nd mode (8 Hz) 3rd mode (12 Hz)

Fig. 10. Measured vibration envelopes (horizontal scale enlarged by a factor of 20 for visibility).

The shape of the first vibration mode at 5 Hz may be expected for a structure of this type. The higher vibration mode shapes are less predictable since they are more sensitive to local variations in the structural properties. These higher modes are therefore also more likely to be able to indicate any changes in stiffness caused by damage or degradation of a structure.

Testing 3D Monitoring

Taking advantage of appropriate photogrammetric procedures and processes, further tests were carried out of the same model to demonstrate the 3D deformation measurement system. The second camera was introduced, and cameras rearranged to achieve appropriately convergent images. Both cameras' external triggers were connected to the shaker table's control system so that they would both be triggered simultaneously. The same motion as in the 2D test was reapplied to the model. Following data capture, the images were processed as before using the blur-measurement algorithm. The steps described in the section *Measurement in 3D* for determining the camera's orientations were followed, and 3D coordinates generated. Fig. 11(a) shows the results from the repeated test which are similar in form to those measured in the first test (Fig. 10).

Detecting Structural Changes

To assess the potential for detecting structural changes using the measured image data, a further test was designed using the same model structure. As shown in Fig. 12, the structure was modified by adding mass to the structure on the fourth level. The test was repeated with the first three mode shapes being captured. Fig. 11(b) shows that the change in the dynamic response of the modified structure can be appreciated by a change in the measured vibration envelope. In particular, more significant three-dimensional changes are observed at the higher modes.

The second modification involved substituting two vertical members with replacements that had part of their cross section cut away (Fig. 12). By reducing the cross-sectional area of the member, the stiffness was reduced. This is a similar effect to the failure of welds in a steel structure, which would result in a loss of stiffness. Changes can be observed in the locations of nodes and antinodes, the positions where the amplitude is smallest and largest. In a practical setting, identifying a change in the vibration envelope when one was not expected would trigger further investigation as to the underlying cause, possibly prompting repair work (Kasinos et al., 2015). Testing was repeated again and results are presented in Fig. 11(c).

It is interesting to note how the analysis of the unmodified model (Fig. 11(a)) reveals a motion which is essentially planar with all the three modes of vibration (5, 8 and 12 Hz); while the two modifications (Figs. 11(b) and (c)) induce some significant torsional effects. Such changes in orientation of the vibration envelope may not ordinarily be detectable with conventional single-axis accelerometers.

Discussion

This paper demonstrates the potential for using controlled blurred images to monitor structural tests using off-the-shelf low-cost equipment and digital photogrammetry. It may be used for a wide range of applications where imaging hardware provides sufficient spatial and temporal resolution. The proposed solution further extends the capabilities of

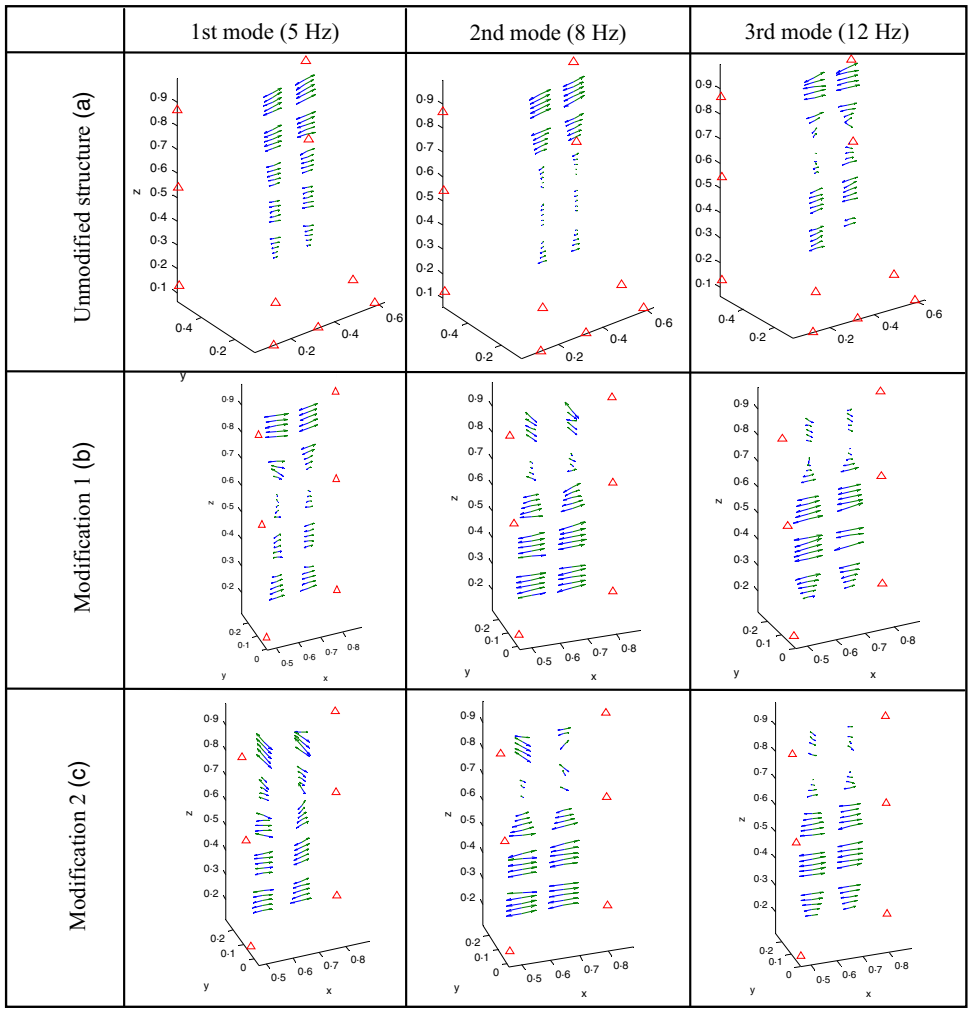

Fig. 11. Measured change in vibration envelope from structural modifications. Blue/green vectors represent individual target displacements, whilst red triangles represent control points. (a) Upper row: unmodified structure. (b) Middle row: modification 1 – the addition of a mass. (c) Lower row: modification 2 – reducing member stiffness.

photogrammetric monitoring by allowing vibration patterns to be identified without the requirement of high imaging speed sensors, which are expensive.

Assessing the Accuracy of the System

An important question is always the accuracy, and this was assessed in another series of simplified tests. Individual targets were mounted directly to the table surface. Since the table motion could be accurately recorded by laser displacement gauges and accelerometers, these results can be directly compared with the recorded motion. Various different amplitudes and target sizes were tested.

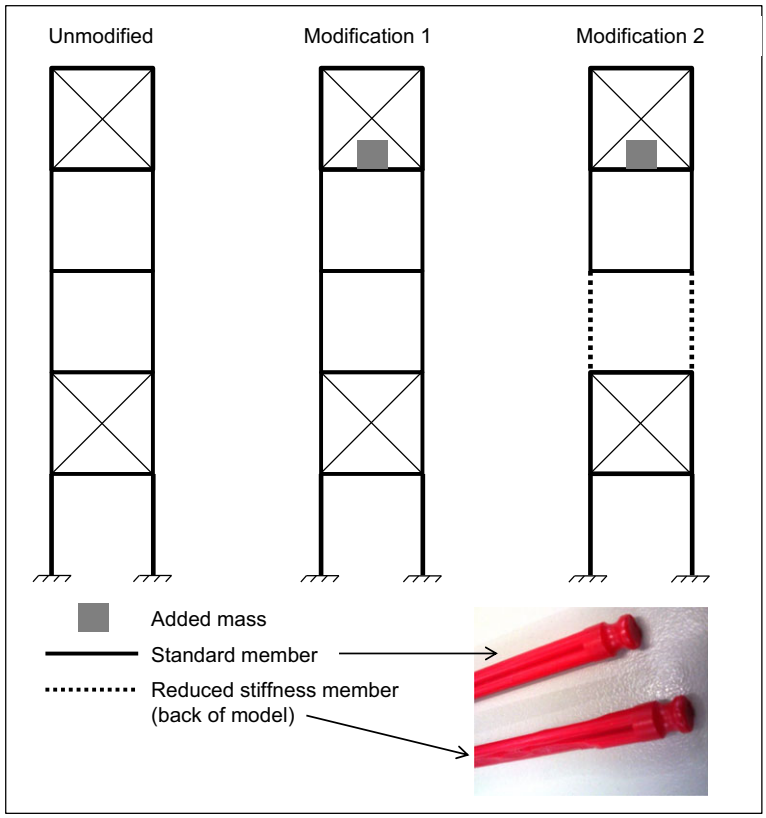

FIG. 12. Modifications made to the model structure, firstly by the addition of a mass on the structure's fourth level and secondly by also reducing the stiffness of members between levels two and three.

Results for errors between the laser displacement gauge measurements and the image-based distance measurements are given in Fig. 13. A standard deviation of $\pm 0{\cdot}158$ mm was observed, with a mean error of just $-0{\cdot}115$ mm for a camera-to-object distance of 1 m. Using a 95% confidence interval, the measured distances are considered accurate to within 0·38 mm. In the image space at this scale, this represents 1·43 pixels at the 95% confidence level. Whilst the accuracy of the current measurement algorithm, when expressed in pixels, is poorer than conventional target-measurement algorithms such as weighted centroid or ellipse fitting, images are obtained at the sensor's highest resolution without having to consider the imaging frequency limitation.

The Nikon D80 cameras have a sensor resolution of 10·2 Mpixel, at which resolution they were found to have a maximum continuous rate of 3 fps. These sensors would be limited to recording vibrations of less than 1·5 Hz at their maximum resolution due to the Nyquist sampling theorem. Utilising the proposed method using blurred imagery, these sensors demonstrated the ability to measure the amplitude and shape of the dynamic response of structures at a frequency of 12 Hz. This approach also allows this to be achieved very efficiently, using a minimum number of images and sensors. Tests have demonstrated how the approach may be used to identify the changes in the vibration

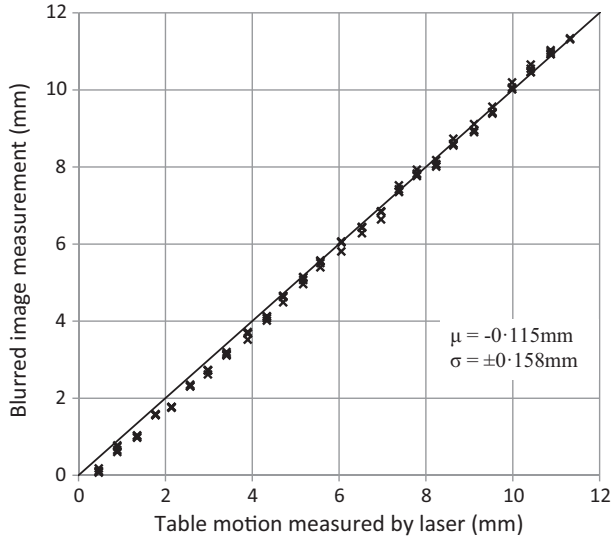

Fig. 13. Results of accuracy assessment comparing laser displacement gauge measurements and blurred image measurements.

envelope of structures, which in turn may be used to identify structural changes, such as the presence of localised damage.

The photogrammetric arrangement makes possible the monitoring of displacements to assess static properties of the structure as well as dynamic ones. Although it is feasible to calculate absolute displacements from acceleration measurements by double integration, the result usually exhibits a drift and alternative sensors are normally necessary for monitoring static structural properties. The arrangement of image sensors and targets makes possible recording of overall displacements of a structure for assessment of the structure's static properties.

Imaging sensors have been used for monitoring vibrations in the conventional way by recording displacement–time history, from which frequency information can be identified using the discrete Fourier transform (Choi et al., 2011; Helfrick et al., 2011; Warren et al., 2011). This monitoring requires cameras with higher speeds at the cost of lower image resolutions. It is possible to improve measurement accuracy by "zooming-in" on a single target, but the advantage of multiple monitoring points would be lost. The advantage of a very high number of monitoring points is of particular interest in the dynamic case. Maintaining a larger image scale allows the higher number of monitoring points to be utilised, thus reducing undesirable interpolation.

Control of the image acquisition time and knowledge of the anticipated motion frequency is necessary to ensure that an appropriate shutter speed is selected. A shutter speed which is too short results in recorded motion that does not conform to the sinusoidal vibration pattern. In practice, relatively fast motion can be easily measured as the camera shutter speed can be adjusted and the image exposure will remain acceptable. The shutter speed can be extended for slower vibration motions, but this may result in images being unacceptably overexposed. In case studies, neutral density filters have been used to reduce image exposure, allowing shutter speeds of the order of seconds to be used. Vibrations with a period of a second have been recorded successfully, but possible frequencies are limited by the imaging system.

While many techniques for interpreting dynamic response make use of frequency information, the proposed approach is frequency independent, rather emphasising spatial measurement of the vibration envelope. The acceleration time history from accelerometer data would usually be used for the identification of multiple frequencies in broadband excitation. When used with frequency-selective excitation, direct spatial measurement of the vibration envelope exhibits nodes, antinodes and shape curvature that can be used for dynamic assessment (Abdel Wahab and de Roeck, 1999). Although only a sinusoidal function has been used in this study to simulate the blur of the target, other functions could be used, depending on the particular regime of motion expected for the structure under observation.

For measurement in 3D, it was recognised that difficulties in target matching exist and how they were overcome has been described. In many static structural testing scenarios, the deformation shape of a structure is relatively easy to predict, since the structure usually deforms in the direction of the applied load, and the use of one-dimensional gauges is often suitable. Out-of-plane movement is more likely to be encountered during dynamic testing, since excited vibration modes could be longitudinal, transverse or torsional. Therefore, 3D monitoring, such as that presented here, may be desirable in more dynamic testing cases. Triaxial variants of accelerometers are also available, but each sensor is upgraded at added cost and more data-acquisition channels are needed, whilst each individual photogrammetric target is relatively inexpensive.

Accelerometers are more sensitive than the proposed image-based approach. Their high sensitivity and frequency information allows the detection of vibrations of very low amplitude and high frequency. When photogrammetry is used for monitoring structural tests it is often commented that traditional contact gauges are known to be more accurate, and are usually used to assess the accuracy of the photogrammetric measurement system (Yoneyama et al., 2005; Rönnholm et al., 2009). However, the cost of an individual accelerometer is high, and extensive cable infrastructure and data-monitoring hardware is required. Since individual accelerometers add significant cost to a monitoring system, as well as time to install, fewer sensors are usually possible than the image-based approach used here. When determining modal shapes it is desirable to reduce the interpolation necessary between monitoring points by increasing their number (Carden and Fanning, 2004).

If employed for monitoring outdoors, the approach in this paper could clearly be affected by factors such as poor weather. Active targets built from high-intensity light-emitting diodes (LEDs) have been discussed by Wahbeh et al. (2003) to allow improved monitoring during hours of darkness and in dull weather. The image-processing algorithm used in this research is likely to be successful on this kind of similar images; this may be an area for future investigation. Other sensors that do not rely on line-of-sight capabilities are not without their own difficulties, and Battista et al. (2011) commented on experiencing missing data due to cable infrastructure problems.

Conclusion

This paper has presented a novel approach to identifying vibration patterns in civil engineering structures using long-exposure images, in which the targets appear blurred because of the motion of the structure. Photogrammetry has already demonstrated its use for monitoring of structural tests where hardware has sufficient imaging speed. The proposed approach aims to directly record the envelope of sinusoidal vibration, rather than instantaneous deformed shapes. This allows sensors with higher image resolutions to be

used and at smaller scale in the field environment. Laboratory tests demonstrate the high quantity of measurements that can be achieved with only a few sensors, and the accuracy of the measurements has been assessed.

The data collected using the blurred-image approach has been compared with traditional dynamic-monitoring instruments. It has also been demonstrated how the approach can be used to detect structural changes in a series of model structures. The new frequency-independent approach expands the capabilities of existing sensors which have otherwise had their applications restricted by their imaging frequency.

REFERENCES

Abdel Wahab, M. M. and de Roeck, G., 1999. Damage detection in bridges using modal curvatures: application to a real damage scenario. *Journal of Sound and Vibration*, 226(2): 217–235.

Banham, M. R. and Katsaggelos, A. K., 1997. Digital image restoration. *IEEE Signal Processing Magazine*, 14(2): 24–41.

Battista, N. de, Westgate, R. and Koo, K. Y., 2011. Wireless monitoring of the longitudinal displacement of the Tamar Suspension Bridge deck under changing environmental conditions. In *Sensors and Smart Structures Technologies for Civil, Mechanical, and Aerospace Systems* (Ed. M. Tomizuka). SPIE, 7981: 798110–15.

Benning, W., Lange, J., Schwermann, R., Effkemann, C. and Gortz, S., 2004. Monitoring crack origin and evolution at concrete elements using photogrammetry. *International Archives for Photogrammetry, Remote Sensing and Spatial Information Sciences*, 35(B5): 678–683.

Boracchi, G., Caglioti, V. and Giusti, A., 2007. Ball position and motion reconstruction from blur in a single perspective image. *14th IEEE International Conference on Image Analysis and Processing*, Modena, Italy. 87–92.

Brownjohn, J. M. W., 2011. Structural health monitoring: examples and benefits to structure stakeholders. *The Structural Engineer*, 89(9): 24–26.

Carden, E. P. and Fanning, P., 2004. Vibration based condition monitoring: a review. *Structural Health Monitoring*, 3(4): 355–377.

Chandler, J. H. and Clark, J. S., 1992. The archival photogrammetric technique: further application and development. *Photogrammetric Record*, 14(80): 241–247.

Choi, H.-S., Cheung, J.-H., Kim, S.-H. and Ahn, J.-H., 2011. Structural dynamic displacement vision system using digital image processing. *NDT & E International*, 44(7): 597–608.

Chopra, A. K., 2007. *Dynamics of Structures: Theory and Application to Earthquake Engineering*. Third edition. Pearson/Prentice Hall, Upper Saddle River, New Jersey, USA. 876 pages.

Clough, R. W. and Penzien, J., 2003. *Dynamics of Structures*. Third edition. Computers and Structures, Berkeley, California, USA. 752 pages.

Cooper, M. A. R. and Robson, S., 1990. High precision photogrammetric monitoring of the deformation of a steel bridge. *Photogrammetric Record*, 13(76): 505–510.

Harvey, B., 2008. Testing and monitoring of structures: traps for the unwary. *Structural Engineer*, 86(20): 22–24.

Helfrick, M. N., Niezrecki, C., Avitabile, P. and Schmidt, T., 2011. 3D digital image correlation methods for full-field vibration measurement. *Mechanical Systems and Signal Processing*, 25(3): 917–927.

Jurjo, D., Magluta, C., Roitman, N. and Goncalves, P., 2010. Experimental methodology for the dynamic analysis of slender structures based on digital image processing techniques. *Mechanical Systems and Signal Processing*, 24(5): 1369–1382.

Kasinos, S., Palmeri, A. and Lombardo, M., 2015. Using the vibration envelope as damage-sensitive feature in composite beam structures. *Structures*, 1: 67–75.

Luhmann, T., Robson, S., Kyle, S. and Harley, I., 2006. *Close Range Photogrammetry: Principles, Techniques and Applications*. Whittles, Dunbeath, Scotland. 528 pages.

Maas, H.-G., 1998. Photogrammetric techniques for deformation measurements on the reservoir walls. *IAG Symposium on Geodesy for Geotechnical and Structural Engineering*, Eisenstadt, Austria. 319–324.

McCarthy, D. M. J., Chandler, J. H. and Palmeri, A., 2013. Monitoring dynamic structural tests using image deblurring techniques. In *Key Engineering Materials. 10th International Conference on Damage Assessment of Structures* (Ed. B. Basu), Dublin, Ireland. 932–939.

McCarthy, D. M. J., Chandler, J. H. and Palmeri, A., 2014. 3D case studies of monitoring dynamic structural tests using long exposure imagery. *International Archives of Photogrammetry, Remote Sensing and Spatial Information Sciences*, 40(5): 407–411.

OLASZEK, P., 1999. Investigation of the dynamic characteristic of bridge structures using a computer vision method. *Measurement*, 25(3): 227–236.

PALMERI, A. and LOMBARDO, M., 2011. A new modal correction method for linear structures subjected to deterministic and random loadings. *Computers & Structures*, 89(11–12): 844–854.

PSIMOULIS, P. A. and STIROS, S. C., 2008. Experimental assessment of the accuracy of GPS and RTS for the determination of the parameters of oscillation of major structures. *Computer-Aided Civil and Infrastructure Engineering*, 23(5): 389–403.

ROBERTS, G. W., MENG, X. and DODSON, A. H., 2004. Integrating a global positioning system and accelerometers to monitor the deflection of bridges. *Journal of Surveying Engineering*, 130(2): 65–72.

RŐNNHOLM, P., NUIKKA, M., SUOMINEN, A., SALO, P., HYYPPÄ, H., PŐNTINEN, P., HAGGRÉN, H., VERMEER, M., PUTTONEN, J., HIRSI, H., KUKKO, A., KAARTINEN, H., HYYPPÄ, J. and JAAKKOLA, A., 2009. Comparison of measurement techniques and static theory applied to concrete beam deformation. *Photogrammetric Record*, 24(128): 351–371.

SIEBERTH, T., WACKROW, R. and CHANDLER, J. H., 2014. Motion blur disturbs – the influence of motion-blurred images in photogrammetry. *Photogrammetric Record*, 29(148): 434–453.

THOMAS, H. and CANTRÉ, S., 2009. Applications of low-budget photogrammetry in the geotechnical laboratory. *Photogrammetric Record*, 24(128): 332–350.

WAHBEH, A. M., CAFFREY, J. P. and MASRI, S. F., 2003. A vision-based approach for the direct measurement of displacements in vibrating systems. *Smart Materials and Structures*, 12(5): 785–794.

WANG, S., GUAN, B., WANG, G. and LI, Q., 2007. Measurement of sinusoidal vibration from motion blurred images. *Pattern Recognition Letters*, 28(9): 1029–1040.

WARREN, C., NIEZRECKI, C., AVITABILE, P. and PINGLE, P., 2011. Comparison of FRF measurements and mode shapes determined using optically image based, laser, and accelerometer measurements. *Mechanical Systems and Signal Processing*, 25(6): 2191–2202.

YITZHAKY, Y., BOSHUSHA, G., LEVY, Y. and KOPEIKA, N. S., 2000. Restoration of an image degraded by vibrations using only a single frame. *Optical Engineering*, 39(8): 2083–2091.

YONEYAMA, S., KITAGAWA, A., KITAMURA, K. and KIKUTA, H., 2005. Deflection distribution measurement of steel structure using digital image correlation. *SPIE*, 5880: 58800G 1–8.

Résumé

La photogrammétrie a été utilisée dans le passé pour surveiller les tests en laboratoire de structures de génie civil au moyen de multiples capteurs imageurs. Cela s'est avéré concluant, cependant la détection de vibrations lors de tests dynamiques reste un défi, car on utilise le plus souvent des caméras à haute fréquence ce qui entraîne une dégradation de la résolution des images et de la précision. Pour surmonter cette limitation, une nouvelle approche a été envisagée, consistant à effectuer des mesures dans des images floues obtenues avec un long temps d'exposition. Le mouvement de la structure est obtenu à partir d'images individuelles que le mouvement a rendues floues, indépendamment de la fréquence d'acquisition. Un algorithme spécialement conçu détermine ensuite le mouvement de chaque point de mesure. Les techniques photogrammétriques permettent de déterminer le mouvement d'un modèle de structure pour différentes fréquences d'excitation et de recréer l'enveloppe de vibration en 3D. Cette approche est testée et utilisée pour identifier des changements dans la réponse aux vibrations d'un modèle.

Zusammenfassung

Mit Hilfe der Photogrammetrie wurden bereits Labortests von Baukörpern mit Hilfe von mehreren bildbasierten Sensoren überwacht. Dies war erfolgreich, aber die Erkennung von Vibrationen bei dynamischen Strukturtests ist eine viel größere Herausforderung, da sie meist von Hochgeschwindigkeitskameras abhängt, die eine geringere Bildauflösung und reduzierte Genauigkeiten besitzen. Um diese Einschränkung zu umgehen, wird ein neuer Ansatz vorgestellt, der auf Messungen in verwaschenen Bildern aus Aufnahmen mit langer Belichtungszeit basiert. Die Bewegung eines Baukörpers wird in individuellen Bewegungsunschärfebildern unabhängig von der Bildgeschwindigkeit erfasst. Ein maßgeschneiderter Algorithmus bestimmt daraus die

Bewegung jedes Messpunktes. Mit Hilfe photogrammetrischer Techniken wird die Bewegung eines Baukörpermodells in Abhängigkeit von verschiedenen Anregungsfrequenzen erfasst und die Einhüllende der Vibration in 3D bestimmt. Der Ansatz ist getestet und wird verwendet, um Änderungen im Antwortverhalten des Modells hinsichtlich der Vibration festzustellen.

Resumen

La fotogrametría, usando sensores basados en imágenes, se ha utilizado en el pasado para controlar pruebas de laboratorio de estructuras de ingeniería civil. Esto ha sido un éxito, pero la detección de vibraciones durante las pruebas dinámicas estructurales ha demostrado ser más difícil, ya que por lo general dependen de cámaras de alta velocidad y a menudo implica una menor resolución de imagen y una menor precisión. Para superar esta limitación, se ha ideado un nuevo enfoque para tomar mediciones de las imágenes borrosas en las fotografías de larga exposición. El movimiento de la estructura es capturado en imágenes individuales borrosas debido al movimiento independientemente de la velocidad de formación de imágenes. Un algoritmo de medida determina entonces el movimiento de cada punto de medición. Mediante técnicas de fotogrametría, se capta el movimiento del modelo de estructura respecto a diferentes frecuencias de excitación y su envolvente de vibraciones recreada en 3D. El método se pone a prueba y se utiliza para identificar los cambios en la respuesta a la vibración del modelo.

摘要

基于摄影测量原理之多影像传感器系统,已常用于土木结构实验室测试监测,且相当成功。但是在动态结构测试之振动检测时,由于所需采用之高速摄像机,经常图像分辨率相对较低,导致精度降低,因而更具挑战性。

为了克服这个限制,本研究提出一个新方法,使用长曝光照片中之模糊图像。结构体之运动由各个模糊图像中撷取,而无需依赖摄像速度。使用一个针对此一问题之算法,可以确定每个测量点的移动。使用摄影测量技术,结构模型相对于不同激发频率的运动可由而在三维空间重建。本方法业经测试,可用于识别模型的振动响应变化。